

# Different Magnetic Field Topologies in Black Hole MAD Accretion Disk Simulations

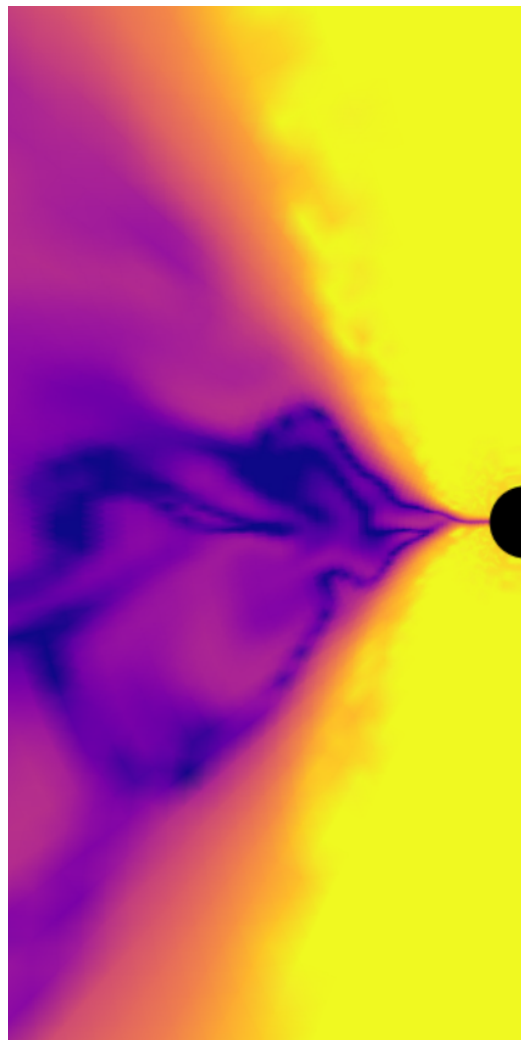
Mário Raia Neto

Federal University of São Carlos

São Carlos, Brazil

Email: [mrneto@estudante.ufscar.br](mailto:mrneto@estudante.ufscar.br) or [mraianeto@gmail.com](mailto:mraianeto@gmail.com)

April 14, 2025



# Internal report of the course: Numerical simulations of accretion discs

Professors: Miljenko Cemeljic and Debora Lančová

Report: Different magnetic field topologies in black hole MAD accretion disk simulations

Student: Mário Raia Neto (from Federal University of São Carlos, Brazil)

email: mrneto@estudante.ufscar.br or mraianeto@gmail.com

## Abstract

Understanding the impact of magnetic field topology on the evolution of black hole accretion disks is essential for interpreting high-energy astrophysical phenomena such as jet formation and relativistic outflows. This work presents a comparative study of two different magnetic configurations—dipolar and multipolar—in the context of Magnetically Arrested Disks (MADs), using two-dimensional general relativistic magnetohydrodynamic (GRMHD) simulations carried out with the `iHarm3d` code. Both setups are based on a modified Fishbone-Moncrief torus in Kerr spacetime, where vector potentials define distinct initial magnetic field structures. We analyze within a low resolution simulation, the time evolution of key physical fluxes—mass accretion rate, magnetic flux, angular momentum flux, and energy extraction efficiency—measured near the event horizon. The results show that dipolar configurations lead to a more stable and efficient MAD state, whereas multipolar topologies generate irregular accretion patterns and lower energy extraction.

## Contents

<b>1</b>	<b>Introduction</b>	<b>2</b>
<b>2</b>	<b>General Relativistic Magnetohydrodynamics</b>	<b>3</b>
2.1	GRMHD Formulation . . . . .	3
2.2	Numerical Implementation: HARM and iHARM3D . . . . .	3
2.3	Astrophysical Context . . . . .	3
<b>3</b>	<b>Torus setups</b>	<b>4</b>
<b>4</b>	<b>Results and discussion</b>	<b>5</b>
4.1	Single magnetic field loop . . . . .	5
4.2	Double magnetic field loop . . . . .	7
<b>5</b>	<b>Conclusions</b>	<b>8</b>
<b>A</b>	<b>About GRMHD simulations with <code>iHarm3d</code> (a step-by-step tutorial)</b>	<b>8</b>
A.1	Obtaining <code>iHarm3d</code> . . . . .	8
A.2	Compiling . . . . .	8
A.3	Starting up a simulation . . . . .	9
A.4	Obtaining the basic plots . . . . .	9
A.4.1	Some customization . . . . .	9
A.5	Obtaining a in depth analysis . . . . .	9
A.5.1	The "KEL" error . . . . .	9
A.6	About 3d simulations . . . . .	9
<b>B</b>	<b>Further comments and hardware</b>	<b>10</b>
B.1	Machine One: Samsung 300E4A . . . . .	10
B.2	Machine Two: HP G42 Notebook . . . . .	10
<b>References</b>		<b>10</b>

## 1 Introduction

The study of black hole accretion disks, particularly in regimes dominated by strong magnetic fields, is fundamental to the understanding of relativistic jet formation, energy extraction, and black hole feedback in active galactic nuclei and X-ray binaries. In such environments, general relativistic magnetohydrodynamics (GRMHD) simulations serve as a powerful tool to investigate the nonlinear interplay between fluid dynamics, magnetic fields, and spacetime curvature.

One of the most widely adopted equilibrium models for initializing GRMHD simulations is the Fishbone-Moncrief torus [FM76], which describes a stationary, axisymmetric, pressure-supported disk orbiting a Kerr black hole [Wal84]. This configuration allows for controlled insertion of magnetic fields, facilitating the development of the magnetorotational instability (MRI) [BH91] and the transition to the Magnetically Arrested Disk (MAD) state [TNM11]. In the MAD regime, the accretion flow is strongly influenced by accumulated magnetic flux near the event horizon, which can modulate the efficiency of angular momentum and energy extraction, most notably through the Blandford-Znajek mechanism [TPM86].

In this context, the topology of the initial magnetic field plays a central role in determining the system's evolution. Dipolar and multipolar magnetic field geometries, for example, can lead to markedly different disk dynamics, stability conditions, and energy output. Yet, the detailed effects of such configurations remain an active area of research, especially considering their influence on the structure of the MAD state and its observational signatures.

This report investigates the dynamical differences that arise from two distinct magnetic field configurations—single and double magnetic loop structures—embedded within an initially identical Fishbone-Moncrief torus. Using the `iHarm3d` code we perform 2D GRMHD simulations to quantify how each topology influences key accretion disk properties. The analysis includes time-resolved diagnostics of mass accretion rate, magnetic flux, angular momentum transport, and energy extraction.

## 2 General Relativistic Magnetohydrodynamics

The Fishbone-Moncrief torus [FM76] is a stationary, axisymmetric solution describing a pressure-supported perfect fluid in the Kerr spacetime [Wal84]. It serves as a widely used initial condition for GRMHD simulations of black hole accretion, particularly in the study of Magnetically Arrested Disks (MADs) [? ]. The Kerr metric in Boyer-Lindquist coordinates is given by:

$$ds^2 = - \left( 1 - \frac{2Mr}{\Sigma} \right) dt^2 - \frac{4Mar \sin^2 \theta}{\Sigma} dt d\phi + \frac{\Sigma}{\Delta} dr^2 + \Sigma d\theta^2 + \left( r^2 + a^2 + \frac{2Ma^2r \sin^2 \theta}{\Sigma} \right) \sin^2 \theta d\phi^2, \quad (1)$$

with  $\Sigma = r^2 + a^2 \cos^2 \theta$  and  $\Delta = r^2 - 2Mr + a^2$ . Assuming constant specific angular momentum  $\ell = -u_\phi/u_t$ , the relativistic Euler equation yields an effective potential:

$$W = \ln |u_t| - \int \frac{dp}{\rho h}, \quad (2)$$

which defines equipotential surfaces. The torus extends from a pressure maximum to an inner cusp near the ISCO, enabling accretion if perturbed.

To model realistic flows, toroidal magnetic fields are seeded via a vector potential, leading to low plasma beta ( $\beta = p/p_m$ ), favoring MRI development [BH91]. The magnetic flux threading the horizon defines the MAD regime through [TNM11]:

$$\phi_{\text{BH}} = \frac{1}{2\sqrt{\dot{M}}} \int_{r=r_H} \sqrt{-g} |B^r| d\theta d\phi. \quad (3)$$

**GRMHD Formulation.** In GRMHD, the conservation laws of mass and energy-momentum in curved spacetime are:

$$\nabla_\mu (\rho u^\mu) = 0, \quad \nabla_\mu T^{\mu\nu} = 0, \quad (4)$$

where  $T^{\mu\nu} = T_{\text{fluid}}^{\mu\nu} + T_{\text{EM}}^{\mu\nu}$  includes both fluid and electromagnetic stress-energy. The electromagnetic part in ideal MHD can be rewritten as [Kom99]:

$$T_{\text{EM}}^{\mu\nu} = b^2 u^\mu u^\nu + \frac{1}{2} b^2 g^{\mu\nu} - b^\mu b^\nu, \quad (5)$$

with the magnetic field four-vector  $b^\mu$  derived from the dual Faraday tensor. The induction equation follows from the homogeneous Maxwell equation and reads in 3+1 form:

$$\partial_t (\sqrt{-g} B^i) = -\partial_j \left[ \sqrt{-g} (b^j u^i - b^i u^j) \right], \quad (6)$$

supplemented by the no-monopole constraint  $\partial_i (\sqrt{-g} B^i) = 0$ .

**Numerical Implementation: HARM and iHARM3D.** The HARM code [GMT03] and its modern extension iHARM3D<sup>1</sup> solve the GRMHD system via conservative finite-volume methods. The evolution equations are written as:

$$\partial_t (\sqrt{\gamma} U) + \partial_i (\sqrt{\gamma} F^i) = \sqrt{\gamma} S, \quad (7)$$

where  $U$  and  $F^i$  include mass, momentum, energy, and magnetic fluxes, and the spacetime geometry is incorporated via the lapse  $\alpha$ , shift  $\beta^i$ , and the spatial metric determinant  $\gamma$  [DZZBL07, Por17]. Primitive-to-conserved variable conversion is analytical, but the inverse requires numerical root finding [NGMDZ06].

**Astrophysical Context.** The dynamics of such systems are extensively discussed in accretion theory literature, e.g., [KFM08], and are foundational to jet-launching models and black hole feedback mechanisms. For a comprehensive treatment of Kerr black holes, see [TPM86, Wal84].

---

<sup>1</sup> Available at <https://github.com/atchekho/iHarm3d>

### 3 Torus setups

First of all, due to computational limitations described in appendix B, the grid resolution <sup>2</sup> was changed into a new grid with dimensions given by,

```

1 /* GLOBAL RESOLUTION */
2 #define N1TOT 128
3 #define N2TOT 32
4 #define N3TOT 1

```

Secondly, the option "mad type = 1" was selected within the "param.dat" file located in the main directory and then the program was compiled (following the procedure described in Appendix A). This choice defines that the poloidal vector potential in the accretion disk should be described as follows:

$$A_\phi = \frac{\rho_{av}}{\rho_{max}}. \quad (8)$$

The definition of the shape of the magnetic field line loops is contained in the file "problem.c" within the "torus" directory. Specifically, starting from line 264, we have the following structure:

```

1 if (N3 > 1) {
2     if (mad_type == SANE) {
3         q = rho_av/rhomax - 0.2;
4     } else if (mad_type == RYAN) { //BR's smoothed poloidal in-torus
5         q = pow(sin(th),3)*pow(r/rin,3.)*exp(-r/400)*rho_av/rhomax - 0.2;
6
7     } else if (mad_type == R3S3) { //Just the r^3 sin^3 th term, proposed EHT
8         standard MAD
9         q = pow(r/rin,3.)*rho_av/rhomax - 0.2;
10
11    } else if (mad_type == GAUSSIAN) { //Gaussian-strength vertical threaded field
12        double wid = 2; //Radius of half-maximum. Units of rin
13        q = gsl_ran_gaussian_pdf((r/rin)*sin(th), wid/sqrt(2*log(2)));
14
15    } else if (mad_type == NARAYAN) { //Narayan '12, Penna '12 conditions
16        //Former uses rstart=25, rend=810, lam_B=25
17        double uc = uu_av - uu_end;
18        double ucm = uu_plane_av - uu_end;
19        q = pow(sin(th),3)*(uc/(ucm+SMALL) - 0.2) / 0.8;
20        //Exclude q outside torus and large q resulting from division by SMALL
21        if ( r > rBend || r < rBstart || fabs(q) > 1.e2 ) q = 0;
22
23        //if (q != 0 && th > M_PI/2-0.1 && th < M_PI/2+0.1) printf("q_mid is %.10e\n",
24        ", q);
25    } else {
26        printf("MAD = %i not supported!\n", mad_type);
27        exit(-1);
28    }
29 } else { // TODO How about 2D?
30     q = rho_av/rhomax;
31 }

```

Listing 1: Definition of  $A_\phi$  component in problem.c

However, it is important to note that these definitions are valid only if the simulation is 3D ("if (N3 > 1)"). Notice that the final "else" clause indicates that if the simulation is only 2D, none of the above options will be implemented, except for (27). Therefore, a modification of  $q$  was required in this line of code, such that:

```

1 } else { // TODO How about 2D?
2     q = rho_av/rhomax;
3 }

```

Listing 2: Definition of  $A_\phi$  component in problem.c

to

```

1 } else { // TODO How about 2D?
2     q = pow(sin(th),3)*pow(r/rin,3.)*exp(-r/400)*rho_av/rhomax - 0.2
3 }

```

Listing 3: Definition of  $A_\phi$  component for a single set of magnetic field loops.

which is the "RYAN" case:

$$A_\phi = \sin^3(\theta) \frac{r^3}{r_{in}^3} e^{-\frac{r}{400}} \frac{\rho_{av}}{\rho_{max}} - 0.2. \quad (9)$$

Furthermore, due to the computational limitations described in Appendix B, a modification to the torus scale was necessary. More specifically, in the "param.dat" file located in the main directory, the parameters  $r_{in}$  and  $r_{max}$  were modified as follows:

<sup>2</sup>in parameters.h, inside torus directory.

```

1 # PROBLEM
2 [dbl] rin = 3.0
3 [dbl] rmax = 9.6

```

which is a setup closer to the outer horizon than the original setup when the one download the code.

Two different magnetic field configurations within the accretion disk were then analyzed. The first consists of a single set of magnetic field loops, while the other features two sets of magnetic field loops, respectively.

$$A_\phi = \sin^3(\theta) \frac{r^3}{r_{in}^3} e^{\frac{-r}{400}} \frac{\rho_{av}}{\rho_{max}} - 0.2. \quad (10)$$

e

$$A_\phi = \cos^4(\theta) \sin^3(\theta) \frac{r^3}{r_{in}^3} e^{\frac{-r}{400}} \frac{\rho_{av}}{\rho_{max}} - 0.2. \quad (11)$$

```

1 } else { // TODO How about 2D?
2     q = pow(cos(theta),4)*pow(sin(theta),3)*pow(r/rin,4.)*exp(-r/400)*rho_av/rhomax -
3     0.2;
}

```

Listing 4: Definition of  $A_\phi$  with multiple magnetic field loops inside the accretion disk.

These are the significant modifications to evolve these two different types of MAD accretion disks (beyond those other changes to prevent the errors described in appendix A). After these changes, we are set to begin the simulation.

## 4 Results and discussion

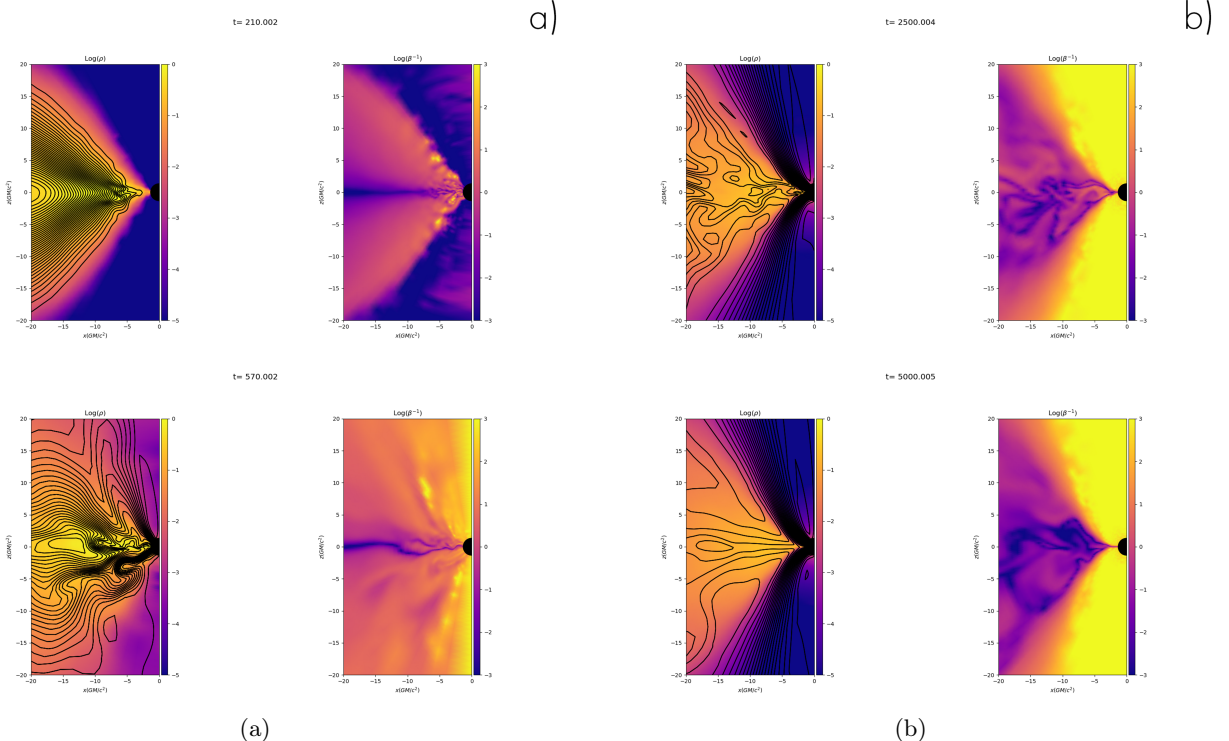


Figure 1: Distributions of logarithmic density  $\log(\rho)$  and plasma beta  $\log(\beta^{-1})$  for dipole poloidal magnetic field loops. In (a), we see the evolution of from  $t = 210$  to  $t = 570$ ; in (b),  $t = 2500$  to  $t = 5000$

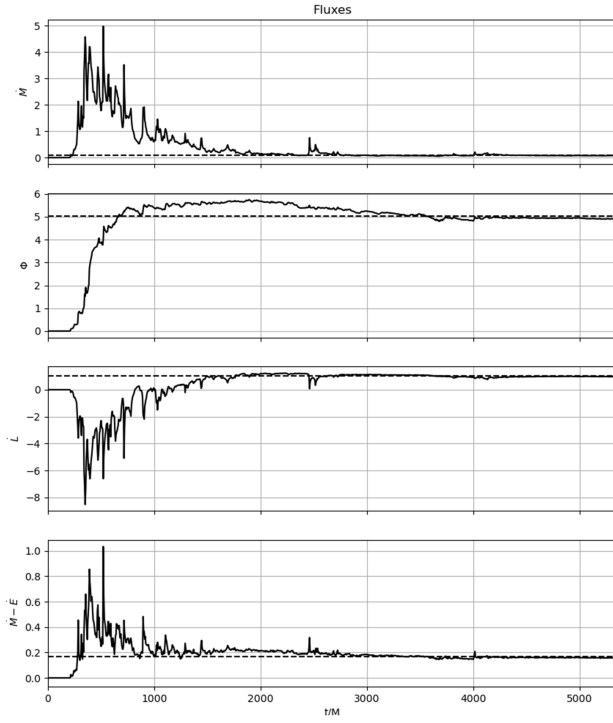


Figure 2: Time evolution of physical fluxes measured near the black hole horizon for the simulation using single set of magnetic field line loops. From top to bottom: mass accretion rate  $\dot{M}$ , magnetic flux  $\Phi$ , angular momentum flux  $\dot{L}$ , and energy extraction efficiency  $(\dot{M} - \dot{E})$ . The dashed lines indicate reference values used for comparison.

**Single magnetic field loop.** In the dipolar configuration (Figure 2), the mass accretion rate  $\dot{M}$  presents an initially transient phase with moderate oscillations, followed by a relatively stable plateau. This stabilization suggests the system reaches a quasi-stationary MAD regime, characterized by the saturation of magnetic flux near the horizon. The associated magnetic flux  $\Phi$  also displays a similar behavior, with a notable increase until a maximum threshold is attained. This is consistent with the accumulation of magnetic field lines at the inner edge of the disk due to the magnetorotational instability (MRI). The angular momentum flux  $\dot{L}$ , carried both by matter and electromagnetic stresses, shows significant correlation with  $\dot{M}$ . This reflects the efficient angular momentum transport mediated by magnetic stresses, particularly the large-scale poloidal magnetic field threading the disk. The relatively smooth behavior of  $\dot{L}$  over time is indicative of an ordered magnetic structure typical of dipolar fields. Finally, the energy extraction efficiency  $\dot{M} - \dot{E}$  increases steadily during the early stages of accretion and saturates around a well-defined value. This behavior is consistent with the Blandford-Znajek mechanism, where energy is extracted from the rotating black hole via magnetic field lines. The dashed lines in the plot serve as fiducial benchmarks, likely representing theoretical expectations or mean values over selected time intervals.

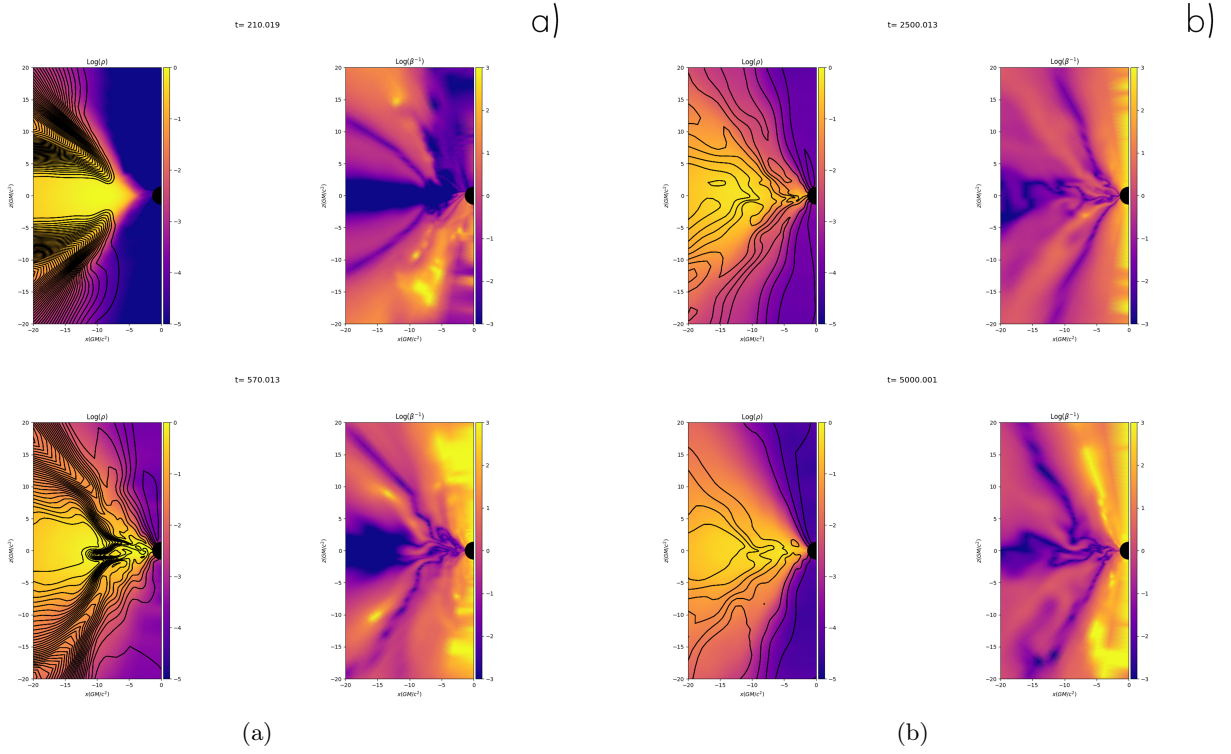


Figure 3: Distributions of logarithmic density  $\log(\rho)$  and plasma beta  $\log(\beta^{-1})$  for dipole poloidal magnetic field loops. In (a), we see the evolution of from  $t = 210$  to  $t = 570$ ; in (b),  $t = 2500$  to  $t = 5000$

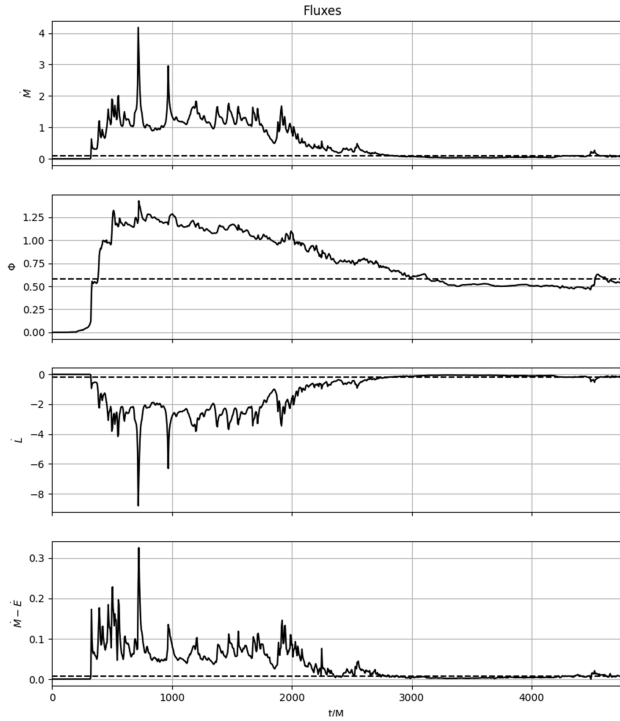


Figure 4: Time evolution of physical fluxes measured near the black hole horizon for the simulation using magnetic multipole loops. From top to bottom: mass accretion rate  $\dot{M}$ , magnetic flux  $\Phi$ , angular momentum flux  $\dot{L}$ , and energy extraction efficiency  $(\dot{M} - \dot{E})$ . The dashed lines indicate reference values used for comparison.

**Double magnetic field loop.** The case with multipolar magnetic field topology (Figure 4) exhibits a markedly different evolution. The mass accretion rate  $\dot{M}$  is less regular, characterized by higher frequency fluctuations and intermittent spikes. This suggests a more chaotic accretion process, possibly due to reconnection events or competing magnetic flux bundles that intermittently inhibit and allow accretion. The magnetic flux  $\Phi$  in this configuration does not reach the same saturation level as in the dipolar case. Instead, the flux shows multiple peaks and valleys, reflecting the complex magnetic field geometry and less efficient channeling of flux toward the horizon. Such behavior points to a non-stationary MAD state with variable degrees of magnetic arrest. The angular momentum flux  $\dot{L}$  displays greater temporal variability,

correlating with the fluctuations in  $\dot{M}$ . The lack of a dominant, coherent poloidal magnetic structure in the multipolar setup likely leads to less efficient angular momentum transport and the emergence of turbulent features. The energy extraction efficiency  $\dot{M} - E$  follows a noisy evolution and does not attain a well-defined asymptotic value, in contrast with the dipolar configuration. This suggests that the multipolar topology is less effective in enabling steady energy extraction from the black hole, likely due to the reduced alignment and connectivity of magnetic field lines with the event horizon.

Comparing both scenarios, we observe that the dipolar topology promotes a more stable and efficient MAD state. The magnetic flux saturates earlier and remains steady, allowing a consistent extraction of angular momentum and energy. In contrast, the multipolar configuration introduces dynamical complexity, variability, and possibly magnetic reconnection episodes that disrupt the coherence of the MAD structure. This analysis highlights the critical role of magnetic field topology in the dynamics of black hole accretion disks. Dipolar configurations facilitate the establishment of ordered MAD states, whereas multipolar setups result in intermittent and less efficient accretion and energy extraction processes.

## 5 Conclusions

This study demonstrates that the magnetic field topology critically influences the evolution of black hole accretion flows in the MAD regime. Simulations with a dipolar magnetic configuration exhibited more stable accretion, higher magnetic flux saturation, and efficient energy extraction, consistent with the establishment of a quasi-stationary MAD state. In contrast, the multipolar configuration led to irregular accretion dynamics and reduced efficiency.

## A About GRMHD simulations with iharm3d (a step-by-step tutorial)

**Obtaining iharm3d.** First of all, in a linux terminal (prefebly a similar distro as the one discribed in appendix B) you should type and install;

```
1 sudo apt-get install libhdf5-mpich-dev
2 sudo apt-get install libgs1-dev
```

then you must donwload the code into your machine,

```
1 git clone https://github.com/AFD-Illinois/iharm3d.git
```

**Compiling.** If everything is set within your system (your machine has C compilers, for instance), then for the compiling you just need:

1. Go to the folder prob/torus, copy any of the "param mad.dat/param sane.dat" to the main folder iharm3d and rename it just as "param.dat".
2. then in the terminal (inside the main folder)

```
1 make distclean
2 make PROB=torus
```

in general, it suffice to compile iharm3d just with,

```
1 make distclean
2 make
```

If everything went well, you should receive a terminal log as in figure 5 (a).

```
raila@raila:~/Downloads/iharm3d$ make distclean
Cleaning build files
Cleaning config files...
raila@raila:~/Downloads/iharm3d$ make
Compiling bounds.c
Compiling coord.c
Compiling current.c
Compiling density.c
Compiling electrons.c
Compiling fixup.c
Compiling fluxes.c
Compiling geometry_utils.c
Compiling io.c
Compiling main.c
Compiling metric.c
Compiling pack.c
Compiling parameters.c
Compiling phys.c
Compiling reconstruction.c
Compiling restart.c
Compiling step.c
Compiling timing.c
Compiling to_par.c
Compiling problem.c
Linking harm
Completed build of prob: torus
CFLAGS: -O3 -fno-mudflap -O3 -march=native -mtune=native -fno-omit-frame-pointer -funroll-loops
```

(a)

```
raila@raila:~/Downloads/iharm3d$ ./iharm
Invalid MIT-MAGIC-COOKIE-1 key
Invalid MIT-MAGIC-COOKIE-1 key
*****
*                                         IHARM3D
*                                         Gammie, McKinney & Toth ApJ 569:444, 2003
*                                         B S Prather
*                                         G N Wong
*                                         B Ryan
*                                         C Gallo
*                                         C P Gamble
*                                         S M Ressler
*
*                                         SYNTAX
*                                         -p /path/to/param.dat
*                                         -o /path/to/output/dir
*****
Parameter file read
No restart file: error 2
Initial conditions generated
iharm: /home/raila/.iharm3d
```

(b)

Figure 5: (a)iharm3d compiling process; (b) starting a simulation.

**Starting up a simulation.** The process of copying the parameter.dat file into the main directory establishes the main parameters for the simulation, and that is why it must be placed in the main directory. Then, after the compiling process, you will notice that some other folders have appeared as well. Then, you should type in the terminal,

```
1 ./harm
```

and the simulation will start (just like figure 5 (b) ).

**Obtaining the basic plots.** After a simulation run, the outputs will reside in the "dumps" folder in the main directory. Inside the main directory, open a terminal and write:

```
1 python3 script/analysis/simple/basic_analysis.py -p script/analysis/simple/
params_analysis.dat
```

Automatically, a "plots" folder will be created and the simulation resultant plots (just like the ones in section 4) will be generated.

#### A.4.1 Some customization

Open the folder script/analysis/simple. Inside this folder you will encounter two files the "basic analysis.py" script and the "params analysis.dat".

Inside the "basic analysis.py" script, you can:

- Change the color scheme of the plot in the very definition of the torus plot function (try change 'jet' to 'plasma'):

```
1 def analysis_torus2d(dumpval, cmap='jet', vmin=-5, vmax=0, domain =
[-50,0,-50,50], bh=True, shading='gouraud'):
2     plt.clf()
```

- Modify the domain of the plot in the very definition of the torus plot function (try change [-50,0,-50,50] to [-20,0,-20,20]):

```
1 def analysis_torus2d(dumpval, cmap='jet', vmin=-5, vmax=0, domain =
[-50,0,-50,50], bh=True, shading='gouraud'):
2     plt.clf()
```

- Change how many magnetic field lines will be shown in the plots (Ln 235) (try change nlines=40 to nlines=20):

```
1 plotting_bfield_lines(ax1,B[Ellipsis,0],B[Ellipsis,1],nlines=40)
```

**Obtaining a in depth analysis.** Beyond the basic script within the "simple" directory, there are much more to be extracted from the dump file. In particular, the fluxes plots from section 4 were generate by the tutorial in the following.

Inside the main directory, open a linux terminal and type

```
1 python3 script/analysis/eht_analysis.py dumps 0
```

If everthing went fine, you should receive a file with a name similar as **eht out xxxx.p**. But, if this isn't the case, and you are receiveing a error with a "key" called "KEL", then you must change some files as described in the following section A.5.1.

In the same terminal, and after receiving the eht out xxxx.p file, you should type

```
1 python3 script/analysis/eht_plot.py eht_out_0.0_5345.004918098228.p Fluxes
```

#### A.5.1 The "KEL" error

The KeyError: 'KEL' probably happens because the Python analysis code (like eht analysis.py or hdf5 to dict.py) expects the 'KEL' variable to exist inside the HDF5 dump files, but it isn't found. Moreover, "KEL" is the electron internal energy per unit mass, added as an extra primitive variable when electron physics is enabled (define ELECTRONS 1) in parameters.h file inside torus folder.

**To circumvent this, one should open the hdf5 to dict.py and change "KEL" to "KEL0", "KEL1", "KEL2" or "KEL3", since these are the key correct names.**

**About 3d simulations.** In the parameters.h, inside torus directory the one can setup a new grid with dimensions given by,

```
1 /* GLOBAL RESOLUTION */
2 #define N1TOT 128
3 #define N2TOT 32
4 #define N3TOT 4
```

For the  $N3TOT > 1$ , the code understands that we are about to simulate MHD in a 3d grid. 3d simulations will not be discussed here in this report, but the compiling process and the plotting process is the same, except that in the "params analysis.dat" the one should change as,

```

1 # Problem dimension, must be 3 or 2 (NOTE: if PROB is set to bondi, analysis script
   by default assumes NDIMS to be 2)
2 NDIMS 2

to

1 # Problem dimension, must be 3 or 2 (NOTE: if PROB is set to bondi, analysis script
   by default assumes NDIMS to be 2)
2 NDIMS 3

```

Therefore, when the one uses the "basic analysis.py" script, it is possible to see the disk accretion both in equatorial and a polar slices (xz and xy)

## B Further comments and hardware

All the simulations of this report were done within a five days time run using two notebooks:

### Machine One: Samsung 300E4A.

1. **Distribution:** Linux Mint 22 Wilma (based on Ubuntu 24.04 Noble)
2. **Desktop Environment:** Cinnamon 6.2.9
3. **Kernel:** 6.8.0-47-generic (64-bit)
4. **GCC Compiler:** v13.2.0
5. **Architecture:** x86\_64
6. **Type:** Laptop
7. **Manufacturer:** Samsung
8. **Model:** 300E4A
9. **Motherboard:** Samsung (FAB1)
10. **BIOS/UEFI:** Phoenix v09QA (11/02/2012)
11. **CPU Model:** Intel Core i5-2450M (Sandy Bridge)
12. **Cores:** 2 physical / 4 logical (Hyper-Threading)
13. **Frequency:** 800 MHz (min) — 3100 MHz (max)
14. **Cache:** L1: 128 KiB, L2: 512 KiB, L3: 3 MiB
15. **Instructions:** avx, sse4.1, sse4.2, vmx, etc.
16. **Current Speed:** 2195 MHz
17. **Bogomips:** 19955
18. **GPU:** Intel 2nd Gen (Gen-6)
19. **Driver:** i915
20. **Resolution:** 1366x656 @ 60Hz
21. **EGL API:** v1.5 (swrast)
22. **OpenGL API:** v4.5 (Mesa 24.0.9)
23. **Renderer:** llvmpipe (LLVM 17.0.6)
24. **Disk:** Seagate ST500LM034-2GH17A (500 GB)
25. **Used Space:** 33.9 GiB / 465.76 GiB (7.3%)
26. **Root (/):** 38.15 GiB (88.8% used) — /dev/sda5
27. **EFI (/boot/efi):** 96 MiB (32.7% used) — /dev/sda1
28. **Swap (file):** 2 GiB — /swapfile
29. **RAM:** 12 GiB (11.6 GiB available)
30. **Shell:** Bash 5.2.21

### Machine Two: HP G42 Notebook.

1. **Distribution:** Linux Mint 22.1 Xia (based on Ubuntu 24.04 Noble)
2. **Desktop Environment:** Xfce 4.18.1
3. **Kernel:** 6.8.0-51-generic (64-bit)
4. **GCC Compiler:** v13.3.0
5. **Architecture:** x86\_64
6. **Type:** Laptop
7. **Manufacturer:** Hewlett-Packard
8. **Model:** HP G42 Notebook PC
9. **Motherboard:** Hewlett-Packard 1425 (v54.57)
10. **BIOS:** HP vF.37 (04/07/2011)
11. **CPU Model:** Intel Core i3 M 350 (Westmere)
12. **Cores:** 2 physical / 4 logical (Hyper-Threading)
13. **Frequency:** 933 MHz (min) — 2266 MHz (max)
14. **Current Average:** 1049 MHz (high: 1398 MHz)
15. **Cache:** L1: 128 KiB, L2: 512 KiB, L3: 3 MiB
16. **Instructions:** sse, sse2, sse3, ssse3, sse4.1, sse4.2, nx, pae, ht
17. **Bogomips:** 18089
18. **GPU:** Intel Gen-5.75 (IronLake)
19. **Driver:** i915
20. **Resolution:** 1366x768 @ 60Hz
21. **EGL API:** v1.5 (crocus, swrast)
22. **OpenGL API:** v4.5 (compat: 2.1), Mesa 24.0.9
23. **Renderer:** Mesa Intel HD Graphics (IronLake)
24. **Disk:** Samsung HM321HI (298.09 GiB)
25. **Used Space:** 21.88 GiB / 298.09 GiB (7.3%)
26. **Root (/):** 236.31 GiB (9.3% used) — /dev/sda6
27. **EFI (/boot/efi):** 511 MiB (1.2% used) — /dev/sda5
28. **Swap (file):** 4.01 GiB (used: 1.4 GiB — 34.8%) — /swapfile
29. **RAM:** 4 GiB (estimated available: 3.63 GiB)
30. **Shell:** Bash 5.2.21

Although the present hardware is very old and not suitable for running these kinds of simulations, it is still perfectly possible to learn how to execute the simulations and extract information from .h5 files. This step is crucial for anyone intending to begin learning GRMHD numerical simulations.

## References

- [BH91] S.A. Balbus and J.F. Hawley. A powerful local shear instability in weakly magnetized disks. i—linear analysis. *The Astrophysical Journal*, 376:214–233, 1991.
- [DZZBL07] L. Del Zanna, O. Zanotti, N. Bucciantini, and P. Londrillo. An efficient shock-capturing central-type scheme for multidimensional relativistic flows. ii. magnetohydrodynamics. *Astronomy & Astrophysics*, 473(1):11–30, 2007.
- [FM76] L.G. Fishbone and V. Moncrief. Relativistic fluid disks in orbit around kerr black holes. *The Astrophysical Journal*, 207:962–976, 1976.

- [GMT03] C.F. Gammie, J.C. McKinney, and G. Tóth. Harm: A numerical scheme for general relativistic magnetohydrodynamics. *The Astrophysical Journal*, 589(1):444, 2003.
- [KFM08] S. Kato, J. Fukue, and S. Mineshige. *Black-Hole Accretion Disks: Towards a New Paradigm*. Kyoto University Press, 2008.
- [Kom99] S.S. Komissarov. A godunov-type scheme for relativistic magnetohydrodynamics. *Monthly Notices of the Royal Astronomical Society*, 303:343–366, 1999.
- [NGMDZ06] S.C. Noble, C.F. Gammie, J.C. McKinney, and L. Del Zanna. Primitive variable solvers for conservative general relativistic magnetohydrodynamics. *The Astrophysical Journal*, 641:626–637, 2006.
- [Por17] O. et al. Porth. Bhac: A new general relativistic magnetohydrodynamics code for astrophysical applications. *Computational Astrophysics and Cosmology*, 4(1):1, 2017.
- [TNM11] A. Tchekhovskoy, R. Narayan, and J.C. McKinney. Efficient generation of jets from magnetically arrested accretion on a rapidly spinning black hole. *Monthly Notices of the Royal Astronomical Society*, 418(1):L79–L83, 2011.
- [TPM86] K.S. Thorne, R.H. Price, and D.A. Macdonald. *Black Holes: The Membrane Paradigm*. Yale University Press, 1986.
- [Wal84] R.M. Wald. *General Relativity*. University of Chicago Press, 1984.